Polymer Journal (2012) 44, 786–794

www.nature.com/pj

ORIGINAL ARTICLE

Solid-state ^{19}F MAS and $^{1}H \rightarrow {}^{19}F$ CP/MAS NMR study of the phase-transition behavior of vinylidene fluoride–trifluoroethylene copolymers: 2. semi-crystalline films of VDF 75% copolymer

Keitaro Aimi and Shinji Ando

The changes in the crystalline structure and molecular mobility in the semi-crystalline vinylidene fluoride (VDF) and trifluoroethylene (TrFE) copolymer P(VDF_{75}/$TrFE_{25}$) caused by the ferroelectric → paraelectric phase transition were analyzed using variable temperature solid-state ^{19}F magic angle spinning (MAS) and $^{1}H \rightarrow {}^{19}F$ cross polarization/MAS nuclear magnetic resonance spectroscopy in the temperature range of 42–129 °C. The conformational exchange between *trans* and *gauche* at the VDF and VDF–TrFE head-to-head linkage gradually increases at temperatures above 77 °C, and the conformational exchange at the head-to-tail linkage has a key role in the ferroelectric → paraelectric phase transition. The anomalous decrease in the amorphous peak intensities and the presence of a $T_{1\rho}{}^{F}$ value similar to that of the crystalline domain at 122 °C indicate that cooperative motion occurs in both phases just above the transition temperature (T_c). The amorphous domain is assimilated by the crystalline domain upon lowering the temperature from 129 to 85 °C, which significantly increases the crystallinity to below T_c, as indicated by the shape of the spectra, and identical $T_{1\rho}{}^{F}$ and $T_1{}^{F}$ values for the two domains at 85 °C.
Polymer Journal (2012) **44,** 786–794; doi:10.1038/pj.2012.114; published online 13 June 2012

Keywords: ^{19}F NMR; phase transition; vinylidene fluoride–trifluoroethylene copolymers

INTRODUCTION

Vinylidene fluoride (VDF)–trifluoroethylene (TrFE) copolymer (P(VDF_x/$TrFE_{1-x}$)), where x is the VDF molar fraction, is a typical ferroelectric polymer that shows a ferroelectric → paraelectric phase transition, which has garnered much interest in the effort to clarify its mechanism.[1,2] Two types of ferroelectric phases have been reported at room temperature, that is, the low-temperature (LT) and the cooled phase, depending on the VDF content and preparation conditions of the copolymer.[2] In the LT phase, the CF_2 dipoles are arranged in parallel because of the planar zigzag formed by the all-*trans* polymer chains, which is the same arrangement as the PVDF form I (β-form), whereas in the cooled phase, long *trans* segments are connected by irregular *trans–gauche* linkages along their chain axis to form a type of super lattice. However, the stable crystal structure in the high-temperature (paraelectric) phase is hexagonal and is composed of statistically mixed chains with TG^+, TG^-, T_3G^+ and T_3G^- conformations. These chains rotate about their axes via the one-dimensional diffusion of the conformational defects along the chain.

Several reports have shown that lamellar crystals grow in P(VDF/TrFE) films at VDF contents of $x = 0.60$ to 0.82 when annealed at temperatures above the Curie point (T_c). In particular, annealing such polymers at elevated temperatures in the paraelectric phase increases the integrated X-ray diffraction intensities of the 110 and 200 reflections, which correspond to the all-*trans* chains, and sharpen the differential scanning calorimetry (DSC) endotherms observed at T_c.[3–7] The efficient growth of lamellar crystals in the paraelectric phase has been explained using a sliding diffusion model for the polymer chains. For instance, a polyethylene lamellar crystal can thicken at higher pressures through the sliding diffusion of chains within the lamellae in the hexagonal phase. Thick lamellar crystals of polyethylene can only be grown in the hexagonal phase.[8]

In a previous article,[9] we reported changes in the conformation and molecular mobility of single-crystalline (SC) films of P(VDF_{75}/$TrFE_{25}$),[10] observed during the phase transition using solid-state ^{19}F magic angle spinning (MAS) and $^{1}H \rightarrow {}^{19}F$ cross polarization (CP)/MAS nuclear magnetic resonance (NMR) spectroscopy. On the basis of the shape of the spectra and the relaxation parameters of the observed crystalline signals in the ^{19}F NMR spectra, it was determined that the conformation of the VDF–TrFE head-to-tail (H–T) linkage is unchanged up to 92 °C, whereas the VDF chain sequence and VDF–TrFE head-to-head (H–H) linkage undergo conformational exchange above 77 °C, the beginning temperature of the phase transition. This reveals that the VDF–TrFE H–T sequence is the most resistant component in polymer chains to the *trans-gauche* conformational

Department of Chemistry and Materials Science, Tokyo Institute of Technology Ookayama, Meguro-ku, Japan
Correspondence: Professor S Ando, Department of Chemistry and Materials Science, Tokyo Institute of Technology, Ookayama 2-12-1-E4-5, Meguro-ku, Tokyo, Japan.
E-mail: sando@polymer.titech.ac.jp
Received 30 January 2012; revised 12 April 2012; accepted 25 April 2012; published online 13 June 2012

exchange below the phase-transition temperature (Curie temperature, T_c). However, the broad signals attributable to the ferroelectric immobile phase disappeared at approximately the T_c, and all chain sequences that included TrFE units underwent significant conformational exchange. In addition, the $T_{1\rho}{}^F$ values for all the peaks decreased to a single value (ca. 20 ms) at 119 °C, which indicates a uniform, nematic liquid-crystal-like molecular motion accompanied by a full chain rotation occurred at this temperature. The significantly larger $T_{1\rho}{}^F$ values observed for peaks (ca. 20 ms) in the paraelectric phase (119 °C) than those in the amorphous domain (<4 ms) at ambient temperature supports the conclusion that the rotational motion of the polymer chains around their axis is restricted in the paraelectric phase. In this study, we focus on the changes to the molecular motion in the amorphous domain and on the fusion of the crystalline and amorphous domains accompanied by the ferroelectric→paraelectric phase transition in particular. Solid-state NMR enables us to selectively observe either the amorphous or crystalline domains by applying the appropriate pulse sequences.[11–13] Using these techniques, we used variable temperature (VT) ^{19}F MAS NMR measurements to analyze the heating and cooling processes for a semi-crystalline P(VDF$_{75}$/TrFE$_{25}$) system containing a significant amorphous domain.

EXPERIMENTAL PROCEDURES

Samples and DSC measurements

P(VDF$_{75}$/TrFE$_{25}$), and an as-received commercial film (AR film) were supplied by Daikin Kogyo Co. Ltd (Osaka, Japan), dried *in vacuo* at 100 °C and used without further treatment.

DSC experiments were performed using a SEIKO SSS5000 DSC220 instrument (SEIKO, Tokyo, Japan) over the range from 30 to 140 °C at a heating/cooling rate of 5 °C min^{-1}. The phase transition temperatures (T_c) of the AR film were determined to be 129 °C and 78 °C upon heating and cooling, respectively. The melting temperature (T_m) was determined as 150 °C by another DSC measurement at a heating rate of 10 °C min^{-1}.

Nuclear magnetic resonance

Solid-state NMR experiments were conducted on a JEOL EX spectrometer (JEOL, Tokyo, Japan) operating at the resonance frequencies of 282.65 MHz for fluorine and 300.40 MHz for protons using a Chemagnetics APEX ^{19}F/^{1}H dual-tune probe (Fort Collins, CO, USA). Samples were spun at the magic angle at a rate of $\omega_r = 16$ kHz. The fluorine and proton r.f. fields were adjusted to fulfill the Hartmann–Hahn sideband-matching condition, $\omega_{1H} = \omega_{1F} - \omega_r = 83$ kHz. The temperature inside the rotor was calibrated using ethylene glycol absorbed onto tetrakis(trimethylsilyl)silane at the same spinning rate (16 kHz).[14] The ambient probe temperature was estimated to be 68 °C at this spinning rate. The temperature was varied from 42 to 119 °C during the VT measurements. All NMR experiments were conducted under thermal equilibrium conditions at each temperature (signal acquisition began 15 min after setting the temperature). Fluorine chemical shifts are quoted relative to the signal for $CFCl_3$ and were measured via replacement with a liquid sample of C_6F_6 (–163.6 p.p.m.) using an 83 kHz proton decoupling field to correct for the Bloch–Siegert effect.[15] The samples were packed at the center of the rotor with 2.5-mm thickness along the axis to ensure the homogeneity of the r.f. fields and sample temperature. The number of acquisitions was 32 for all experiments, except the delayed CP experiments.

Figure 1 shows the NMR pulse sequences used in this study. The spin-lattice relaxation times in the rotating ^{19}F ($T_{1\rho}{}^F$) frame were measured via variable spin-lock time experiments. The relevant pulse sequence is depicted in Figure 1a. The spin-lock times (t_{SL}) varied from 0.01 to 20 ms. The delayed CP sequence was used to selectively observe signals with long spin–spin relaxation times, T_2, which generally corresponded to the mobile (amorphous) phase. The pulse sequence is shown in Figure 1b. The contact time (t_{CP}) and delay time (τ) were set to 0.2 ms and 0.5 ms, respectively. The additional spin-lock period was used to measure the $T_{1\rho}{}^F$ of the mobile phase. However, the

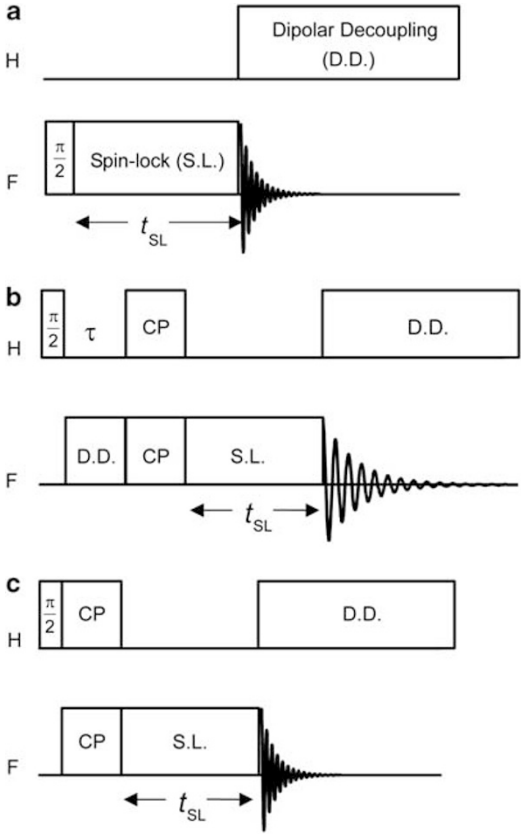

Figure 1 Pulse sequences for (**a**) the variable spin-lock time measurements for $T_{1\rho}{}^F$, (**b**) delayed CP followed by variable spin-lock time measurements for the selective observation of $T_{1\rho}{}^F$ in the amorphous domain, and (**c**) short CP followed by variable spin-lock time measurements for the selective observation of $T_{1\rho}{}^F$ in the crystalline domain. An ordinary CP experiment without using spin-lock time measurements, t_{SL}, is shown in (**c**).

$T_{1\rho}{}^F$ measurement for the rigid (crystalline) phase was performed using a short CP followed by a spin-lock period, as shown in Figure 1c. This short contact time ($t_{CP} = 0.1$ ms) was used to eliminate the signals from the amorphous phase.

RESULTS AND DISCUSSION

Selective observation of the amorphous and crystalline domains

Figure 2a (top) shows the direct polarization (DP) ^{19}F MAS NMR spectra ($t_{SL} = 0$ ms) with broadband ^{1}H decoupling for an AR film at 42 °C. The high-frequency (from –88 to –130 p.p.m.) and low-frequency (from –195 to –210 p.p.m.) signals correspond to the ^{19}F nuclei in the CF_2 and CHF groups of the P(VDF$_{75}$/TrFE$_{25}$), respectively. This spectrum is significantly different from that of the crystal-like (SC) film,[9] which has broad components that are predominant in both the high- and low-frequency regions. On the basis of the ^{19}F solution spectra reported by Mabboux and Greason,[16] the three peaks at –88.4 (peak 1_{am}, CF_2–CH_2–CF_2–CH_2–CF_2), –102.2 (peak 3_{am}, CF_2–CH_2–$\underline{C}F_2$–CHF–CF_2) and –109.2 p.p.m. (peak 4_{am}, CF_2–CH_2–$\underline{C}F_2$–CF_2–CH_2) were assigned to the CF_2 groups in the VDF region. The subscript 'am' for the peak numbers indicates a signal from the amorphous region. Peak 5_{am} at –119.5 p.p.m. (CF_2–CHF–CF_2–CHF–CF_2) and peak 6_{am} at –127.0 p.p.m. (CH_2–CF_2–CF_2–CHF–CH_2) were assigned to the CF_2 adjacent to a CHF. Peak 7_{am} at –195.8 p.p.m. was assigned to the –CF_2–CH_2–CF_2–CH_2–(CH$\underline{F}$–CF_2)–CF_2–CH_2–CF_2–CH_2– sequences, where the VDF and TrFE units are linked H–H. The other marked CHF peak, observed at –203.7 p.p.m.

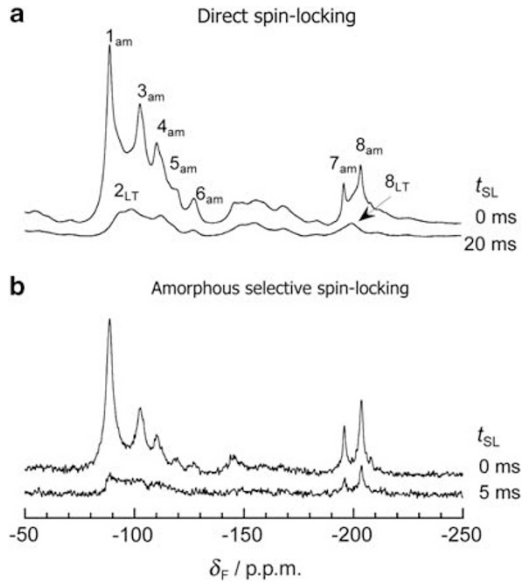

Figure 2 (**a**) Direct polarization ^{19}F MAS NMR spectrum of the AR film (top), and the crystalline-selective spectrum observed by spin-locking for 20 ms (bottom). (**b**) Amorphous-selective spectrum of the AR film before (top) and after a spin-lock of 5 ms spectrum (bottom).

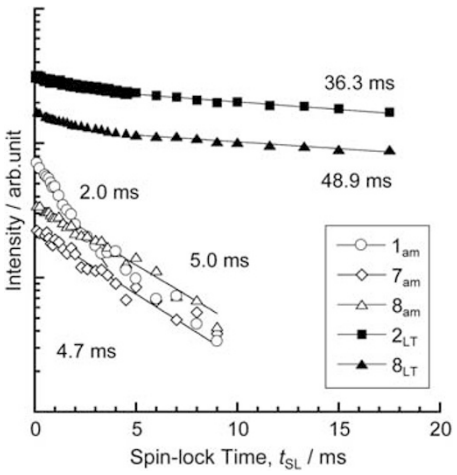

Figure 3 Spin-lock time dependence of the ^{19}F signal intensity for the selectively observed amorphous and crystalline signals at 68 °C with $T_{1\rho}^{F}$ values obtained using single- or double-exponential functions. The pulse sequences shown in Figure 1b and Figure 1c are used for the amorphous (1_{am}, 7_{am} and 8_{am}) and crystalline signals (2_{LT} and 8_{LT}), respectively.

(peak 8_{am}), was assigned to the –CF_2–CH_2–CF_2–CH_2–(CF_2–CHF)–CF_2–CH_2–CF_2–CH_2– sequences, where VDF and TrFE units are linked H–T. Figure 2a (bottom) shows the crystalline selective spectrum obtained using the spin-lock pulse sequence ($t_{SL} = 20$ ms, Figure 1a). Peaks 2_{LT} and 8_{LT} were assigned to the VDF chain sequence and the H–T linkage in the all-*trans* crystalline domain, respectively.[9] The subscript 'LT' for the peak numbers indicates signals from the LT phase in the crystalline domain. The effective suppression of the sharp amorphous signals indicates that the molecular mobility of the amorphous domain is significantly different from that of the crystalline domain. This situation is similar to the PVDF homopolymer.[12] In addition, the amorphous selective spectra obtained using the delayed CP pulse sequence, both with and without spin-locking ($t_{SL} = 0$ and 5 ms), are shown in Figure 2b. The intensities of the broad crystalline signals in Figure 2a (top; i.e., 2_{LT} and 8_{LT}) were significantly reduced in Figure 2b. The ^{19}F magnetization decay for peaks 1_{am}, 7_{am} and 8_{am} observed by delayed CP followed by variable ^{19}F spin-lock experiments are shown in Figure 3. The $T_{1\rho}^{F}$ values obtained by fitting the decays using either a single- or double-exponential function were incorporated into the figure. As peak 1_{am} overlapped the remnant of the crystalline signals, two relaxing components were observed with the longer component containing the spin diffusion from the crystalline to the amorphous domains. As shown in Figure 2b, peak 1_{am} almost entirely disappeared after spin-locking for 5 ms, whereas the two CHF resonances (peak 7_{am} and 8_{am}) were still observed. This was expected based on the longer $T_{1\rho}^{F}$ components of the latter signals (4.7 and 5.0 ms) relative to the former signal (2.0 ms). These results suggest that the molecular mobility was larger at the VDF sequence near the spin-lock frequency (100 kHz) than the CHF units. Furukawa *et al.*[17] reported that the frequency dependence of the relative permittivity (real part, ε', and imaginary part, ε'') for P(VDF$_{65}$/TrFE$_{35}$) showed a wide distribution during heating from 10^3 to 10^8 Hz with a maximum of approximately 10^6 Hz at 40 °C. Ishii *et al.*[18–20] examined the temperature dependence of the line width, second moment and T_1^{H} of P(VDF-TrFE) at VDF contents from 52 to 72% using wide-line proton NMR, and they found a T_1^{H} relaxation process at approximately 30 to 80 °C, which would likely be caused by the motion of the chain backbone in the partially crystalline region. They also suggested that the molecular mobility of the VDF component was different from that of the TrFE component, which may undergo a 180° flip-flop motion. As describe below, peak 7 exhibited a shorter T_1^{F} component than peak 1, which was presumably caused by the rapid motion of the TrFE units. Although it is not easy to infer the dynamics of the local TrFE unit from these ^{19}F NMR measurements, the short relaxation of T_1^{F} may correspond to this flip-flop motion.

The decays of the ^{19}F magnetization for the 2_{LT} and 8_{LT} peaks measured using a short CP followed by a variable spin-lock time experiment at 42 °C are also shown in Figure 3. A short contact time (0.1 ms) was used to reduce the influence of the amorphous domain on the decay of the crystalline signals. However, two $T_{1\rho}^{F}$ components were observed for both peaks (2_{LT} and 8_{LT}), and the shorter components were attributable to the amorphous resonances caused by spectral overlap, that is, to spectral spin diffusion. The $T_{1\rho}^{F}$ values for the crystalline domain were approximately 10 times larger than those of the amorphous domain as shown by the DP spectrum using a long spin lock (Figure 2a (bottom)). We discuss the temperature dependence of the $T_{1\rho}^{F}$ values in both the amorphous and crystalline domains in the following sections to clarify the changes to the molecular mobility within each domain.

VT measurements

Heating process. Figure 4 shows the VT DP ^{19}F MAS NMR spectra of an AR film upon heating. The heights of peaks 1_{am}, 7_{am} and 8_{am} increase continuously over the temperatures from 42 to 114 °C, whereas their half-widths decrease, which confirms the molecular motion in the amorphous domain gradually becomes more vigorous. At 100 °C, a new peak, 7_{HT}, appeared at a higher frequency, separated from peak 7_{am}. This peak was assigned to the H–H linkage in the paraelectric crystalline domain, because its chemical shift agreed well with that observed for the paraelectric phase in the P(VDF$_{75}$/TrFE$_{25}$) SC film from our previous study.[9] However, peak 8_{HT}, assignable to the H–T linkage, appeared at –201.8 p.p.m. and 114 °C. These phenomena are explicable by the initiation of the *trans-gauche*

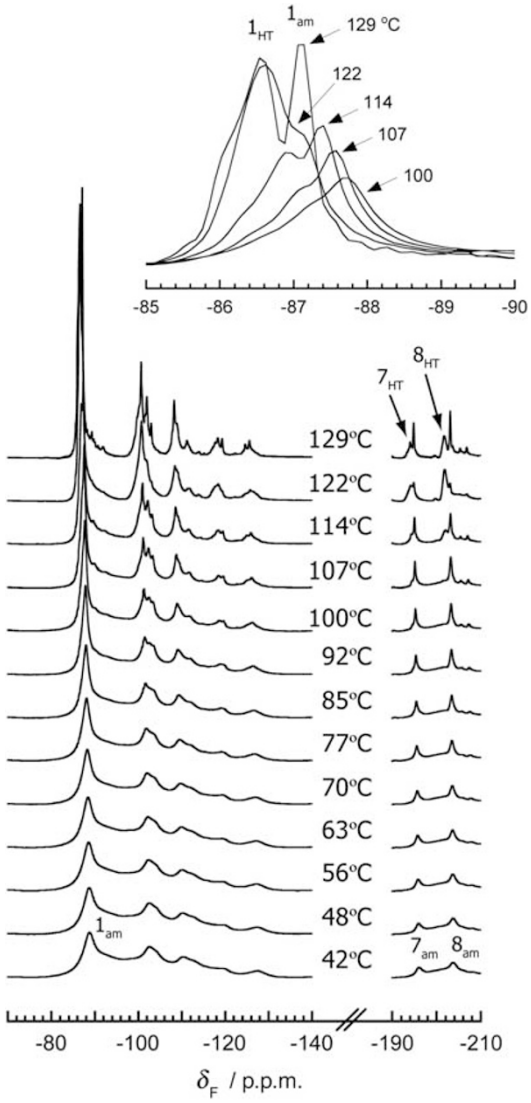

Figure 4 VT DP ^{19}F MAS NMR spectra upon heating. The CF_2 and CHF regions are expanded in this figure. The inset shows the expanded scale for the VDF sequence in the range between 100 and 129 °C.

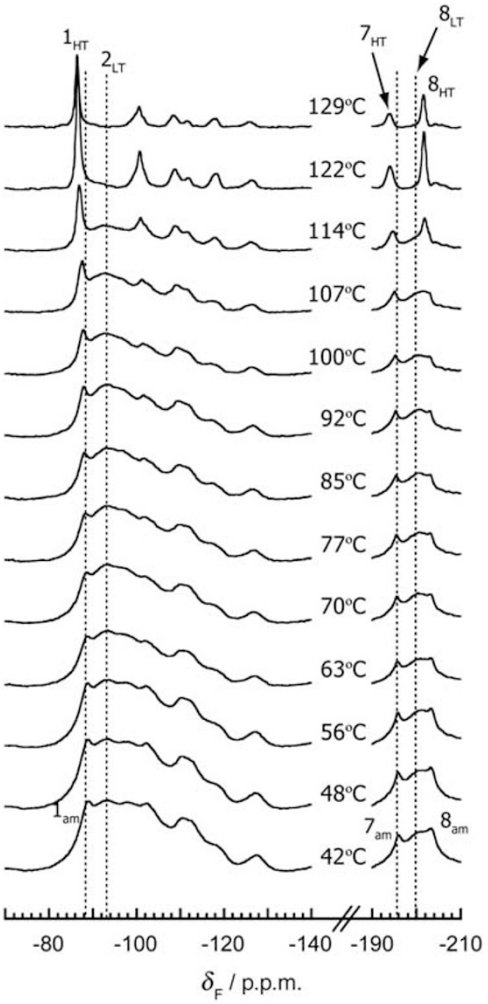

Figure 5 VT ^{1}H→^{19}F CP/MAS NMR spectra upon heating. The contact time used was 0.2 ms for each spectrum.

conformational exchange in the crystalline domain, as previously observed for the SC film.[9] The conformational changes to the VDF chain sequence in the crystalline domain can be recognized in the CP/MAS spectra. Figure 5 shows the VT ^{1}H→^{19}F CP/MAS NMR spectra with a short contact time (0.1 ms) with the AR film upon heating. It should be noted that the small, sharp signals for the amorphous domain (peaks 1_{am}, 7_{am} and 8_{am}) were also observed at the same peak positions in the DP spectrum at 42 °C. Above 77 °C, peak 1_{am} increased in intensity and gradually shifted to higher frequency. Judging by the above findings, the exchange motion in the crystalline domain occurs above 77 °C at the VDF sequence and the H–H linkage, whereas the conformation of the H–T linkage remains stable below 107 °C. The conformational exchange behavior in the crystalline domain of the AR film agrees with that previously observed for the SC film.[9]

Figures 4 and 5 show the signal intensities of peaks 1_{HT} and 8_{HT} increased rapidly between 114 and 129 °C, whereas the intensity of peak 2_{LT} decreased. These results indicate the ferroelectric→paraelectric phase transition occurred in this temperature range, which agrees with the sharp endotherm in the DSC experiments (129 °C, chart not shown). An anomaly in the shape of the spectra was observed at 122 °C in Figure 4. The intensity of peak 1_{am} abruptly decreased, whereas that of peak 1_{HT} increased complimentarily (see the magnified spectra in Figure 4). An increase in peak 1_{HT} was also observed in the short CP spectrum (Figure 5), which suggests that the molecular motion in the crystalline domain slowed abruptly at this temperature. At this point, the intensities of peaks 7_{am} and 8_{am} also decreased in the DP spectrum, whereas those of peaks 7_{HT} and 8_{HT} increased. These phenomena clearly indicate a cooperative motion occurred in both the amorphous and crystalline domains during the phase transition, which slowed and fused the molecular motion in both domains. This anomalous increase in the dielectric constant and slowing of the dielectric relaxation spectra have also been observed for P(VDF/TrFE) at approximately the T_c,[17,21,22] which was explained as a large corrective polarization fluctuation perpendicular to the chain axis. Ohigashi *et al.*[23] reported that the diffuse scattering profile for the hexagonal (002) diffraction of the *TG* and *TG′* units agreed well with the calculated curve assuming rotation in the *TGTG′* sequence. In addition, a larger dielectric relaxation strength was observed for $\varepsilon_{//}$ than $\varepsilon_{\perp}$ (electric field is parallel and perpendicular to the chain axis,

respectively), which was attributed to the flip-flop motion of the *TGTG′* sequence. Moreover, Tanaka *et al.*[24] reported that annealing at just below T_c induced a large growth in the crystalline length along the *c* axis. The slow down and fusion in both the crystalline and amorphous domains observed in this study could have been caused by the propagation of conformational exchanges beyond the interface between the crystalline and amorphous domains, with incorporating conformational kinks into the amorphous domain.

Figure 6 illustrates the changes in the molecular conformation and the motion in both the crystalline and amorphous domains caused by the heat-induced phase transition based on the changes in the VT spectra (Figures 4 and 5). The phase transition was induced as follows. First, the fraction of the conformational exchange increased at the VDF and H–H linkage at 77 °C. Then, the conformational exchange at the H–T linkage became vigorous at over 107 °C. Hence, the H–T linkage had a key role in the phase transition. The cooperative motion occurred in both the amorphous and crystalline domains at the phase-transition temperature of 122 °C. After the completion of the phase transition at 129 °C, peak 1_{am} reappeared with a narrow linewidth (see the magnified spectra). These results indicate that the cooperative motion occurring in both the crystalline and amorphous domains collapsed in the paraelectric phase, and the molecular motion in the amorphous domain became independent from the crystalline domain. ^{19}F relaxation time analyses justify these phenomena as described below.

Figure 7a shows the temperature dependence of the $T_{1\rho}{}^{F}$ values for peaks 1_{am}, 7_{am} and 8_{am} obtained via direct spin-lock experiments (Figure. 1a) upon heating. The values of the shorter $T_{1\rho}{}^{F}$ components for each peak did not change significantly between 56 and 107 °C, despite the tendency of the $T_{1\rho}{}^{F}$ for peak 1_{am} to increase with the temperature. Considering the T_g of this copolymer is less than 0 °C,[21] this phenomenon suggests that the motion at frequencies much higher than 100 kHz become dominant in the amorphous VDF chain sequences at elevated temperatures. As shown in Figure. 7b, the ratio of the shorter $T_{1\rho}{}^{F}$ components began decreasing at 85 °C, whereas the ratio of the longer $T_{1\rho}{}^{F}$ components increased complimentarily, which means that rapid molecular motions, such as the conformational exchange between *trans* and *gauche* conformers in the amorphous domain, were significantly stimulated, and thus the $T_{1\rho}{}^{F}$ values for the shorter relaxation components began increasing above 85 °C. Therefore, the longer components consisted of not only the crystalline domain but also a certain portion of the amorphous domain at temperatures over 85 °C. The temperature dependence of the $T_{1\rho}{}^{F}$ values for the crystalline domain is shown in Figure 7c. These

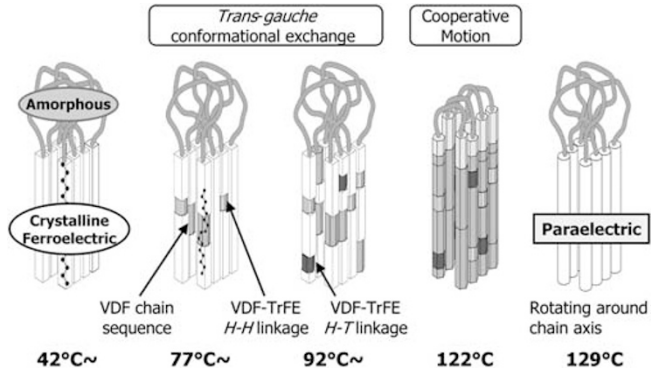

Figure 6 Illustration of the changes in the molecular conformation and motion of the crystalline and amorphous domains caused by the phase transition upon heating (see text).

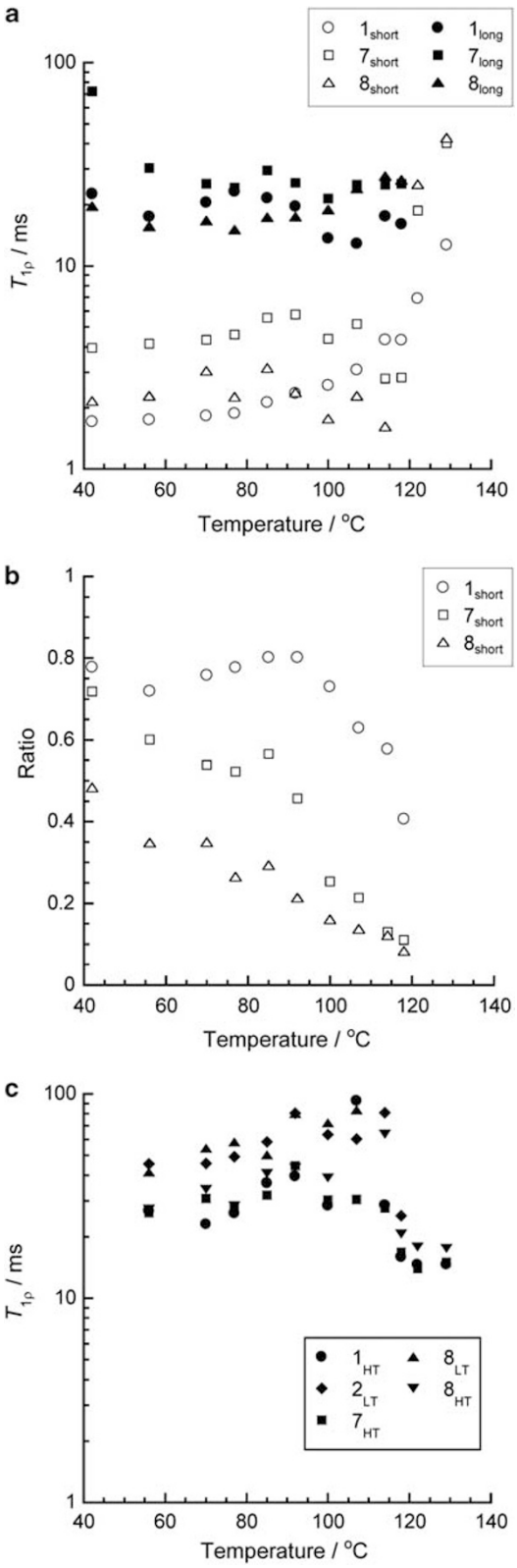

Figure 7 Temperature dependence of (**a**) the spin-lattice relaxation time in the rotating frame, $T_{1\rho}{}^{F}$, obtained by direct spin-lock experiments, (**b**) the ratio of the short components of $T_{1\rho}{}^{F}$, and (**c**) $T_{1\rho}{}^{F}$ from the crystalline signals obtained by short CP followed by a spin-lock period.

values ranged from 20 to 90 ms between 42 and 107 °C. Although these $T_{1\rho}^{F}$ values may have relatively large errors, they indicate an absence of molecular motion at approximately 100 kHz. Note that the $T_{1\rho}^{F}$ values decreased from 25 to 30 ms, to 15 ms, and became identical for all peaks between 114 and 122 °C. As reported in our previous paper,[9] the $T_{1\rho}^{F}$ of the crystalline domain of the SC film abruptly collapsed to a unique value at 119 °C, which indicated a uniform molecular motion involving all of the chain sequences rotating around their chain axis was induced.[2,25,26] The same change in molecular motion occurred in the crystalline domain of the AR film during the phase transition.

Figures 8a and b show the decay of the ^{19}F magnetization in the variable spin-lock experiments at 122 and 129 °C, respectively. All of these decays can be fitted using single-exponential functions. At 122 °C, the crystalline (1_{HT}, 7_{HT}, 8_{HT}) and amorphous (7_{am}, 8_{am}) signals exhibit similar $T_{1\rho}^{F}$ values; however, the $T_{1\rho}^{F}$ of peak 1_{am} is slightly smaller. This finding supports the existence of cooperative motion in both the amorphous and crystalline domains as indicated by the spectral shapes (Figure 4). Similar $T_{1\rho}^{F}$ values (ca. 20 ms) were obtained for peaks 7_{HT} and 8_{HT} at 129 °C as shown in Figure 8b; however, the $T_{1\rho}^{F}$ of peak 1_{HT} was significantly shorter (12 ms) than the others, which indicates the amorphous domain moves more rapidly than the crystalline domain in the paraelectric phase. In addition, the $T_{1\rho}^{F}$ of peak 1_{am} was significantly shorter than those of peaks 7_{am} and 8_{am}, but close to that of peak 1_{HT}, which indicates the molecular mobility of the VDF chain sequence in the amorphous domain is less than that of the TrFE units, and cooperative motion occurs between the crystalline and amorphous domains in the VDF chain sequence.

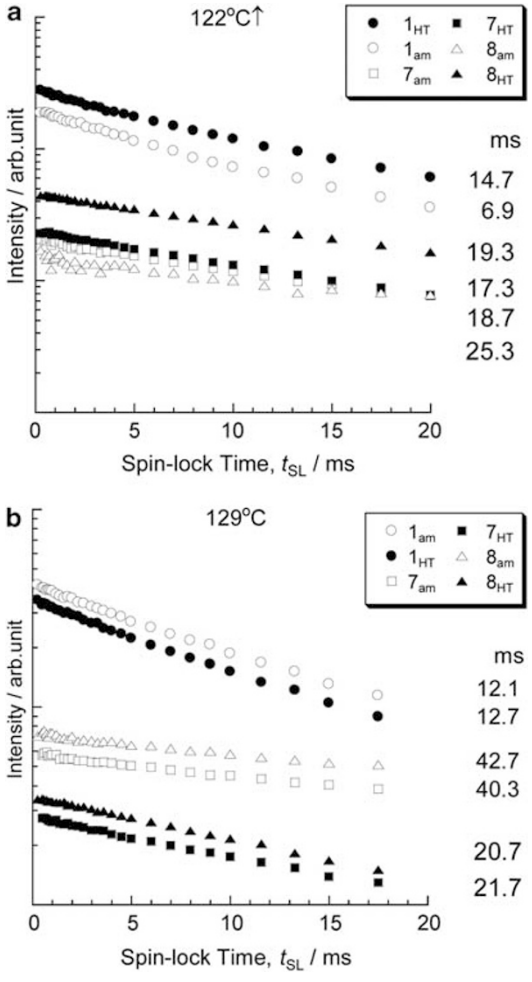

Figure 8 Spin-lock time dependence of the ^{19}F signal intensities observed at (**a**) 122 and (**b**) 129 °C upon heating along with their $T_{1\rho}^{F}$ values.

The temperature dependence of the spin–lattice relaxation times, T_1^F, upon heating is summarized in Table 1. The integrated signal intensity was used for peak 1, which includes both 1_{am} and 1_{HT}. Two decay components were observed for each peak in the temperature range from 42 to 119 °C. Because these T_1^F values were obtained via a DP inversion-recovery pulse sequence, the longer components include contributions from the crystalline domains. The shorter T_1^F components indicate that 20 to 30% of the amorphous phase experienced vigorous motion at several hundreds of MHz at 42 °C. This fast motion presumably corresponds to the conformational exchange between *trans* and *gauche* conformers and the flip-flop of the TrFE units.[18–20] The shorter components of T_1^F gradually increased upon heating from 42 to 100 °C, whereas the longer components decreased. Simultaneously, the ratios of the shorter components increased by up to 40–50% at 100 °C. These facts indicate that the conformational exchange was gradually activated at elevated temperatures. The proportion of the short components in peaks 7_{am} and 8_{am} increased rapidly above 77 °C. In addition, an anomalous increase in T_1^F was observed in the long components of peaks 7 and 8 at 114 °C, and jumped to 0.5 s at 119 °C (only one relaxing component was observed for each peak at this temperature). These facts suggest the rapidly moving TrFE units slowed down at just below the T_c, whereas no significant change occurred in the VDF sequences, which agrees well with the $T_{1\rho}^{F}$ behaviors mentioned above. It should be noted that the anomalous behavior observed for peaks 7 and 8 corroborates the role of the TrFE units as an anchor that prevents full chain rotation just below the T_c upon heating.

Cooling process. Figures 9 and 10 show the DP ^{19}F MAS and ^{1}H→^{19}F CP/MAS NMR spectra, respectively, of the AR film upon cooling. The intensity of the sharp amorphous signal of the VDF chain sequence (peak 1_{am}) decreased between 129 (Figure 5) and 122 °C, and was assimilated into peak 1_{HT}, which decreased in intensity and experienced a low-frequency shift once the temperature was lowered to

Table 1 Temperature dependence of the spin-lattice relaxation times, T_1^F, upon heating

	Short component						*Long component*		
	Peak 1		*Peak 7*		*Peak 8*		*Peak 1*	*Peak7*	*Peak 8*
Temp (°C)	T_1^F/ s	*Ratio*	T_1^F/ s	*Ratio*	T_1^F/ s	*Ratio*	T_1^F/ s	T_1^F/ s	T_1^F/ s
42	0.21	0.29	0.20	0.22	0.22	0.20	1.6	1.6	1.6
56	0.27	0.34	0.12	0.20	0.49	0.38	1.4	1.2	1.5
70	0.20	0.34	0.13	0.21	0.15	0.20	1.2	1.1	1.1
77	0.21	0.39	0.10	0.17	0.23	0.31	1.2	0.95	1.1
85	0.21	0.40	0.14	0.23	0.20	0.31	1.1	0.89	1.0
92	0.22	0.45	0.29	0.45	0.27	0.38	1.0	1.1	1.0
100	0.23	0.48	0.33	0.53	0.30	0.42	1.0	1.1	0.96
107	0.24	0.50	0.36	0.60	0.36	0.56	0.97	1.1	1.1
114	0.40	0.54	0.47	0.87	0.44	0.80	0.95	1.6	1.4
118	0.33	0.59	0.51	1.00	0.51	1.00	0.92		
122	0.58	1.00	0.60	1.00	0.56	1.00			
129	0.49	1.00	0.50	1.00	0.49	1.00			

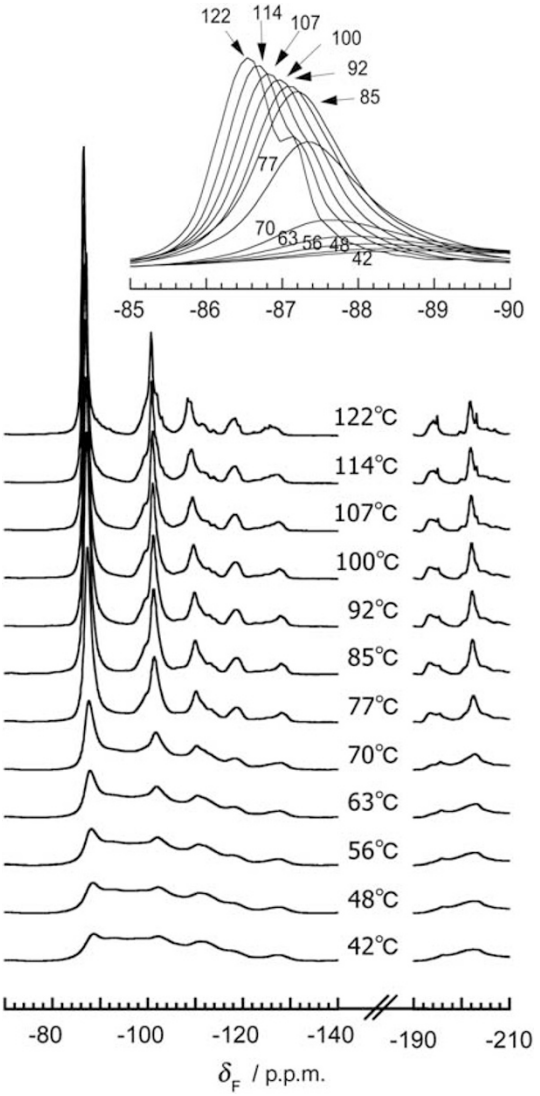

Figure 9 VT DP ^{19}F MAS NMR spectra upon cooling. The inset shows an expansion of the VDF sequence region.

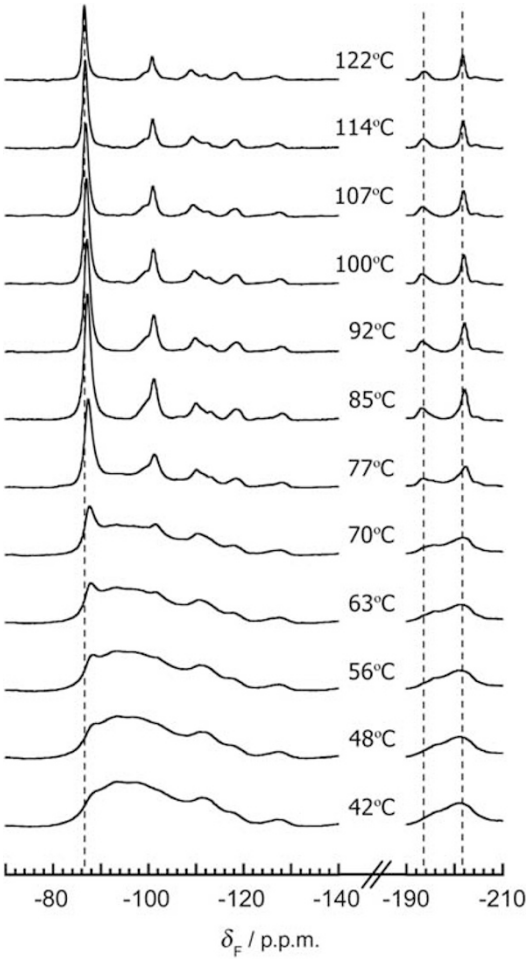

Figure 10 VT ^{1}H→^{19}F CP/MAS NMR spectra upon cooling. The contact time used was 0.2 ms for each spectrum.

85 °C. Simultaneously, the intensity of peak 1_{HT} increased in the short CP spectra, which contrasts the DP spectra and indicates the molecular motion of the VDF chain sequence slowed markedly as the temperature was lowered. The low-frequency shift in peak 1_{HT} corresponded to a decrease in the *gauche* conformer of the VDF chain sequence. Similar spectral changes were observed for the spectral region of CHF fluorines. The sharp amorphous resonances for peaks 7_{am} and 8_{am} weakened in the DP spectra, and significant increases were observed in the crystalline peaks 7_{HT} and 8_{HT} from 122 to 85 °C. These observations demonstrate that the cooperative molecular motion was initiated and spread over the paraelectric crystalline and amorphous domains in this temperature range. In addition, the amorphous domain was gradually assimilated into the crystalline domain where the molecular motion slowed and the number of *gauche* conformers in the VDF sequence and H–H linkage decreased with decreasing temperatures.

The sudden appearance of broad crystalline signals throughout the spectrum at 77 °C in Figure 9 indicates that the transition from the paraelectric to the ferroelectric phases occurred between 85 and 77 °C. This temperature range also matched the transition temperature measured by DSC. Lowering the temperature further promptly decreased the intensities of the sharp signals, and the crystalline signals increased complementarily. The spectral shape measured at 42 °C in the DP spectrum was quite different from the one measured before heating (Figure 4), and the sharp, amorphous resonances were only weakly observed after heating. These findings supports the suggestion that molecular chains containing considerable amounts of the *gauche* conformer in the amorphous domain were gradually incorporated into the crystalline domain, which consisted entirely of the *trans* conformer, by annealing. As the molecular chains underwent vigorous rotational and sliding motions along the chain axis in the hexagonal phase, the annealing procedure significantly improved their arrangement and removed conformational defects via this sliding motion. The spectral changes and $T_{1\rho}^{F}$ measurements (described below) upon cooling suggest the sliding motion was extensively diffused within the amorphous domain in the hexagonal phase.

The changes in the T_1^F values upon cooling are summarized in Table 2. A single relaxation component was observed for each peak, and the T_1^F values were identical for all of the peaks between 122 and 85 °C. These values tended to decrease from 0.60 s at 122 °C to 0.44 s at 85 °C, which implies uniform molecular motion occurred at approximately several MHz in the paraelectric phase and slowed gradually with decreasing temperature. Two relaxation components

Table 2 Temperature dependence of the spin-lattice relaxation times, T_1^F, upon cooling

	Short component						*Long component*		
	Peak 1		*Peak7*		*Peak 8*		*Peak 1*	*Peak 7*	*Peak 8*
Temp (°C)	T_1^F/ *s*	*Ratio*	T_1^F/ *s*	*Ratio*	T_1^F/ *s*	*Ratio*	T_1^F/ *s*	T_1^F/ *s*	T_1^F/ *s*
122	0.60	1.0	0.62	1.0	0.60	1.0			
114	0.59	1.0	0.55	1.0	0.57	1.0			
107	0.53	1.0	0.51	1.0	0.51	1.0			
100	0.50	1.0	0.50	1.0	0.50	1.0			
92	0.45	1.0	0.46	1.0	0.46	1.0			
85	0.43	1.0	0.44	1.0	0.44	1.0			
77	0.45	0.86	0.46	0.84	0.49	0.83	5.53	3.63	4.71
70	0.41	0.61	0.35	0.35	0.45	0.42	2.70	1.83	2.12
63	0.32	0.40	0.31	0.22	0.54	0.32	2.16	1.86	2.32
56	0.29	0.32	0.37	0.22	0.60	0.24	2.29	2.16	2.48
42	0.36	0.25	0.44	0.19	1.05	0.25	2.70	2.83	3.04

were observed below the phase-transition temperature (77–85 °C for cooling) for each peak: the longer T_1^F components attributable to the crystalline domain were over 2 s, and the shorter ones attributable to the amorphous domain continually decreased throughout the phase transition. The proportion of the shorter components promptly decreased to 20–25% at 42 °C after the phase transition, which indicates the conformational exchange motion was frozen, and the polymer chains were in all-*trans* conformation in the ferroelectric phase. The longer T_1^F components at 77 °C are above 3 s, which was significantly longer than those below 70 °C. Although a full understanding of the long T_1^F components was not achieved, they may be related to the changes in the motional mode caused by the termination of the chain rotation. The longer components gradually increased from 77 to 43 °C, which indicated the molecular chains in the crystalline domain stabilized at lower temperatures.

The temperature dependence of $T_{1\rho}^F$ upon cooling is summarized in Table 3. These values for peaks 7_{am} and 8_{am} promptly decrease upon cooling from 129 to 114 °C similarly to those for peaks 7_{HT} and 8_{HT} (Figure 11 and Table 3). In addition, the $T_{1\rho}^F$ value of peak 1_{am} approached those of peaks 7_{HT} and 8_{HT} between 122 and 107 °C. As mentioned above, a decrease in the signal intensities of the amorphous peaks and the increase in those of the crystalline peaks was observed in the DP and short CP spectra, respectively, across the same temperature range. These facts also support that the molecular motion in the amorphous domain slowed and began cooperating with that of the crystalline domain in the paraelectric phase (H–T phase). Upon lowering the temperature to 85 °C, the $T_{1\rho}^F$ values became identical for all peaks (ca. 10 ms), which indicates there was no difference in the molecular mobility at approximately 100 kHz between the amorphous and H–T crystalline phases.

Two $T_{1\rho}^F$ components were observed below the phase transition for all of the peaks. The longer and shorter components correspond to the ferroelectric crystalline and amorphic domains, respectively. The $T_{1\rho}^F$ values of the longer components promptly increased from 77 to 63 °C, which indicates the rotational motion in the paraelectric phase suddenly ended, and the polymer chains all reverted to the *trans* conformer in both the VDF chain sequence and the TrFE units. These conformational changes were also clearly observed in the short contact CP spectra.

Table 3 Temperature dependence of the spin-lattice relaxation time in the rotating frame, $T_{1\rho}^F$, upon cooling

	$T_{1\rho}^F$/ *ms*							
	Peak 1		*Peak 7$_{am}$*	*Peak7$_{HT}$*	*Peak7$_{LT}$*	*Peak 8$_{am}$*	*Peak 8$_{HT}$*	*Peak 8$_{IT}$*
Temp (°C)	*Short*	*Long*						
129			40.3			42.7		
114		13.6	18.7	17.0			17.8	
100		11.5	13.0	12.8			13.5	
92		10.3	10.6	11.2			11.9	
85		9.5	9.2	10.4			10.8	
77	2.6	27.9	5.4		60.0			26.9
70	1.0	36.0	1.7		53.2			47.0
63	2.3	30.3			65.6			39.0

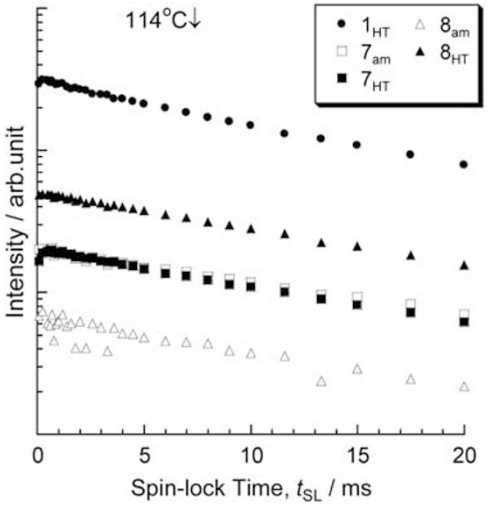

Figure 11 Spin-lock time dependence of the ^{19}F signal intensity at 114 °C upon cooling.

CONCLUSIONS

The changes in the molecular conformation, phase structure and molecular mobility of semi-crystalline P(VDF$_{75}$/TrFE$_{25}$) films containing significant amorphous domains, which were caused by the ferroelectric to paraelectric phase transition, were analyzed using solid-state ^{19}F MAS and ^{1}H→^{19}F CP/MAS NMR. A delayed CP pulse sequence was used to selectively observe signals from the amorphous domain, whereas short CP experiments were used to eliminate the signals from the amorphous domain. The $T_{1\rho}^F$ values of the amorphous signals were estimated to be 2.0 ms for the VDF chain sequence and 4.7–5.0 ms for TrFE units at 42 °C, which suggests a higher molecular mobility occurs for the former in the amorphous domain at approximately 100 kHz.

The VT experiments indicated that the molecular motion in the amorphous domain was closely related to that of the crystalline domain near the phase-transition temperature upon both heating and cooling. The anomalous decrease in the signal intensity of peak 1_{am} and its $T_{1\rho}^F$ value being similar to the crystalline domain at 122 °C indicate a cooperative motion occurred in both phases at the phase-transition temperature. Changes in the conformation and molecular mobility of the crystalline domain in the AR film were practically

identical to those in the SC film: the conformational exchange between *trans* and *gauche* gradually increased in VDF and at the VDF–TrFE H–H linkage with elevating temperatures, and the conformational exchange motion at the H–T linkage induced the phase transition. The amorphous domain was assimilated into the crystalline domain upon lowering the temperature from 129 to 85 °C as shown by the spectral shapes, and identical $T_{1\rho}{}^{F}$ and $T_1{}^{F}$ values for the two domains at 85 °C, which significantly increased the crystallinity below the T_c.

ACKNOWLEDGEMENTS

We thank T Kodani at Daikin Kogyo Co., Ltd. for providing the P(VDF$_{75}$/TrFE$_{25}$) copolymer. We also thank RK Harris, P Avalle, DC Apperley and P Wormald for their help with the measurements and for their discussion.

1 Furukawa, T. Ferroelectric properties of vinylidene fluoride copolymers. *Phase Transitions* **18,** 143–211 (1989).
2 Tashiro, K. in *Ferroelectric Polymers* (ed. Nalwa, H. S.) Ch. 2, 63–181 (Marcel Dekker, New York, 1995).
3 Ohigashi, H. & Koga, K. Ferroelectric copolymers of vinylidenefluoride and trifluoroethylene with a large electromechanical coupling factor. *Jpn J. Appl. Phys.* **21,** L455–L457 (1982).
4 Koga, K. & Ohigashi, H. Piezoelectricity and related properties of vinylidene fluoride and trifluoroethylene copolymers. *J. Appl. Phys.* **59,** 2142–2150 (1986).
5 Koga, K., Nakano, N., Hattori, T. & Ohigashi, H. Crystallization, field-induced phase transformation, thermally induced phase transition, and piezoelectric activity in P(vinylidene fluoride-TrFE) copolymers with high molar content of vinylidene fluoride. *J. Appl. Phys.* **67,** 965–974 (1990).
6 Tanaka, R., Tashiro, K. & Kobayashi, M. Annealing effect on the ferroelectric phase transition behavior and domain structure of vinylidene fluoride (VDF)-trifluoroethylene copolymers: a comparison between uniaxially oriented VDF 73 and 65% copolymers. *Polymer* **40,** 3855–3865 (1999).
7 Barique, M. A. & Ohigashi, H. Annealing effects on the Curie transition temperature and melting temperature of poly(vinylidene fluoride/trifluoroethylene) single crystalline films. *Polymer* **42,** 4981–4987 (2001).
8 Hikosaka, M. Unified theory of nucleation of folded-chain crystals (FCCs) and extended-chain crystals (ECCs) of linear-chain polymers: 2. Origin of FCC and ECC. *Polymer* **31,** 458–468 (1990).
9 Aimi, K., Ando, S., Avalle, P. & Harris, R. K. Solid-state ^{19}F MAS and ^{1}H→^{19}F CP/MAS NMR study of the phase transition behavior of vinylidene fluoride-trifluoroethylene copolymers: 1. Uniaxially drawn films of VDF 75% copolymer. *Polymer* **45,** 2281–2290 (2004).
10 Ohigashi, H., Omote, K. & Gomyo, T. Formation of "single crystalline films" of ferroelectric copolymers of vinylidene fluoride and trifluoroethylene. *Appl. Phys. Lett.* **66,** 3281–3283 (1995).
11 Holstein, P., Harris, R. K. & Say, B. J. Solid-state ^{19}F NMR investigation of poly(vinylidene fluoride) with high-power proton decoupling. *Solid State Nucl. Magn. Reson.* **8,** 201–206 (1997).
12 Wormald, P., Apperley, D. C., Beaume, F. & Harris, R. K. Fluorine-19 solid-state NMR investigation of regiodefective semicrystalline α-poly(vinylidenefluoride). *Polymer* **44,** 643–651 (2003).
13 Hazendonk, P., Harris, R. K., Ando, S. & Avalle, P. The DIVAM sequence: selective excitation of signals from both rigid and mobile domains in a fluoropolymer. *J. Magn. Reson.* **162,** 206–216 (2003).
14 Aliev, A. E. & Harris, K. D. M. Simple technique for temperature calibration of a MAS probe for solid-state NMR spectroscopy. *Magn. Reson. Chem.* **32,** 366–369 (1994).
15 Bloch, F. & Siegert, A. Magnetic resonance for nonrotating fields. *Phys. Rev.* **57,** 522–527 (1940).
16 Mabboux, P. Y. & Gleason, K. K. ^{19}F NMR characterization of electron beam irradiated vinylidene fluoride-trifluoroethylene copolymers. *J. Fluorine Chem.* **113,** 27–35 (2002).
17 Furukawa, T., Ohuchi, M., Chiba, A. & Date, M. Dielectric relaxations and molecular motions in homopolymers and copolymers of vinylidene fluoride and trifluoroethylene. *Macromolecules* **17,** 1384–1390 (1984).
18 Ishii, F., Odajima, A. & Ohigashi, H. Ferroelectric transition in vinylidene-trifluoroethylene copolymer studied by nuclear magnetic resonance method. *Polym. J.* **15,** 875–882 (1983).
19 Ishii, F. & Odajima, A. Proton spin lattice relaxation in vinylidene fluoride/trifluoroethylene copolymer I. vinylidene fluoride. *Polym. J.* **18,** 539–546 (1986).
20 Ishii, F. & Odajima, A. Proton spin lattice relaxation in vinylidene fluoride/trifluoroethylene copolymers II. effects of vinylidene fluoride content upon spin relaxation processes. *Polym. J.* **18,** 547–555 (1986).
21 Koizumi, N., Haikawa, N. & Habuka, H. Dielectric behavior and ferroelectric transition of copolymers of vinylidene fluoride and trifluoroethylene. *Ferroelectrics* **57,** 99–119 (1984).
22 Omote, K., Ohigashi, H. & Koga, K. Temperature dependence of elastic, dielectric, and piezoelectric properties of 'single crystalline" films of vinylidene fluoride trifluoroethylene copolymer. *J. Appl. Phys.* **81,** 2760–2769 (1997).
23 Ohigashi, H., Omote, K., Abe, H. & Koga, K. Chain motions in the paraelectric phase in single crystalline films of vinylidene fluoride and trifluoroethylene copolymer P(VDF/TrFE). *J. Phys. Soc. Jpn.* **68,** 1824–1827 (1999).
24 Tanaka, R., Tashiro, K. & Kobayashi, M. Annealing effect on the ferroelectric phase transition behavior and domain structure of vinylidene fluoride (VDF)–trifluoroethylene copolymers: a comparison between uniaxially oriented VDF 73 and 65% copolymers. *Polymer* **40,** 3855–3865 (1999).
25 Tashiro, K., Takano, K., Kobayashi, M., Chatani, Y. & Tadokoro, H. Structure and ferroelectric phase transition of vinylidene fluoride-trifluoroethylene copolymers: 2. VDF 55% copolymer. *Polymer* **25,** 195–208 (1984).
26 Tashiro, K., Takano, K., Kobayashi, M., Chatani, Y. & Tadokoro, H. Structural study on ferroelectric phase transition of vinylidene fluoride-trifluoroethylene copolymers (III) dependence of transitional behavior on VDF molar content. *Ferroelectrics* **57,** 297–326 (1984).